1-1-2006

Mitochondrial uncoupling protein-4 regulates calcium homeostasis and sensitivity to store depletion-induced apoptosis in neural cells

Sic. L. Chan

Dong Liu

George A. Kyriazis
University of Central Florida

Pamela Bagisyao
University of Central Florida

Xin Ouyang

THE JOURNAL OF BIOLOGICAL CHEMISTRY VOL. 281, NO. 49, pp. 37391–37403, December 8, 2006
Printed in the U.S.A.

Mitochondrial Uncoupling Protein-4 Regulates Calcium Homeostasis and Sensitivity to Store Depletion-induced Apoptosis in Neural Cells*

Received for publication, June 9, 2006, and in revised form, September 7 , 2006 Published, JBC Papers in Press, October 11, 2006, DOI 10.1074/jbc.M605552200

Sic. L. Chan[‡1,2], **Dong Liu**[§1], **George A. Kyriazis**[‡], **Pamela Bagsiyao**[‡], **Xin Ouyang**[§], **and Mark P. Mattson**[‡¶]

From the [‡]*Biomolecular Science Center, University of Central Florida, Orlando, Florida 32816, the* [§]*Laboratory of Neurosciences, Intramural Research Program, NIA, National Institutes of Health, Baltimore, Maryland 21224, and the* [¶]*Department of Neuroscience, Johns Hopkins University School of Medicine, Baltimore, Maryland 21205*

An increase in the cytoplasmic-free Ca^{2+} concentration mediates cellular responses to environmental signals that influence a range of processes, including gene expression, motility, secretion of hormones and neurotransmitters, changes in energy metabolism, and apoptosis. Mitochondria play important roles in cellular Ca^{2+} homeostasis and signaling, but the roles of specific mitochondrial proteins in these processes are unknown. Uncoupling proteins (UCPs) are a family of proteins located in the inner mitochondrial membrane that can dissociate oxidative phosphorylation from respiration, thereby promoting heat production and decreasing oxyradical production. Here we show that UCP4, a neuronal UCP, influences store-operated Ca^{2+} entry, a process in which depletion of endoplasmic reticulum Ca^{2+} stores triggers Ca^{2+} influx through plasma membrane "store-operated" channels. PC12 neural cells expressing human UCP4 exhibit reduced Ca^{2+} entry in response to thapsigargin-induced endoplasmic reticulum Ca^{2+} store depletion. The elevations of cytoplasmic and intramitochondrial Ca^{2+} concentrations and mitochondrial oxidative stress induced by thapsigargin were attenuated in cells expressing UCP4. The stabilization of Ca^{2+} homeostasis and preservation of mitochondrial function by UCP4 was correlated with reduced mitochondrial reactive oxygen species generation, oxidative stress, and Gadd153 up-regulation and increased resistance of the cells to death. Reduced Ca^{2+}-dependent cytosolic phospholipase A2 activation and oxidative metabolism of arachidonic acid also contributed to the stabilization of mitochondrial function in cells expressing human UCP4. These findings demonstrate that UCP4 can regulate cellular Ca^{2+} homeostasis, suggesting that UCPs may play roles in modulating Ca^{2+} signaling in physiological and pathological conditions.

First identified and studied in brown fat cells, where they can dissociate oxidative phosphorylation from respiration and thereby promote heat production, mitochondrial uncoupling proteins (UCPs)[3] are a family of proton carrier proteins located in the inner mitochondrial membrane (1). Five mammalian UCPs, each with distinct tissue distributions, have been identified: UCP1 is expressed primarily in brown fat cells, UCP2 is widely expressed, including in neurons and glial cells, UCP3 is expressed principally in skeletal muscle cells, and UCP4 and UCP5 (also called BMCP1) are expressed in the nervous system (1). The functions of UCPs in neurons have not been established, but, based on their functions in other cell types, they are presumed to modulate the production of ATP and reactive oxygen species (ROS). One recent study showed that UCP5 is present in neurons throughout the brain and that overexpression of UCP5 in cultured neural cell line results in higher state 4 respiration and reduced mitochondrial membrane potential and ROS levels (2). Another study showed that levels of UCP2 are higher in the immature brain and that high levels of UCP2 are associated with increased resistance of neurons to seizures (3), excitotoxicity (4), and ischemia (5). UCP2 expression is induced by ischemic and oxidative damage (3, 5) suggesting that it may protect neurons by functionally uncoupling mitochondria, thereby reducing ROS production. Although the brain-specific UCP4 was discovered more than 5 years ago (6), little is known about its function in neurons.

The intracellular messenger Ca^{2+} regulates many crucial processes, including motility, secretion, gene expression, as well as many of the signaling cascades that drive proliferation, differentiation, and various metabolic reactions. Another major role for Ca^{2+} is in cell death in physiological settings or during injury or diseases (7, 8). The mechanisms that control cellular Ca^{2+} dynamics are complex, with ion channels and pumps in the plasma membrane and endoplasmic reticulum (ER) playing major roles in regulating both rapid and long-term changes in the cytoplasmic free Ca^{2+} concentration ($[Ca^{2+}]_i$). When Ca^{2+} is released from the ER Ca^{2+} store in response to signals that activate receptors coupled to inositol trisphosphate (IP_3) production, the emptying of the ER Ca^{2+} stores triggers Ca^{2+}

* The costs of publication of this article were defrayed in part by the payment of page charges. This article must therefore be hereby marked "*advertisement*" in accordance with 18 U.S.C. Section 1734 solely to indicate this fact.

[1] Both authors contributed equally to this work.

[2] To whom correspondence should be addressed: University of Central Florida, 4000 Central Florida Blvd., Orlando, FL 32816. Tel.: 410-558-8463; Fax: 410-558-8465; E-mail: schan@mail.ucf.edu.

[3] The abbreviations used are: UCP, uncoupling protein; ER, endoplasmic reticulum; ROS, reactive oxygen species; cPLA2, cytosolic phospholipase A2; C_2-ceramide, *N*-acetyl-D-sphingosine; IP_3, inositol trisphosphate; SOCE, store-operated Ca^{2+} entry; SOCC, store-operated Ca^{2+} channel; TRP, transient receptor potential; TG, thapsigargin; RT, reverse transcription; TMRE, tetramethylrhodamine; DHR, dihydrorhodamine 123; DCF, 2,7-dichlorodihydrofluorescein diacetate; BK, bradykinin; CCCP, carbonyl cyanide *m*-chlorophenylhydrazone; AM, acetoxymethyl ester; Rhod-2, dihydrorhodamine-2; VT, vector-transfected; siRNA, small interference RNA; hUCP, human UCP; Gadd153, growth-arrest DNA damage-inducible protein 153; $[Ca^{2+}]_m$, releasable Ca^{2+} from mitochondria; $[Ca^{2+}]_e$, external Ca^{2+} concentration.

influx through La^{3+}-sensitive/nifedipine-insensitive Ca^{2+}-conducting channels in the plasma membrane, a process that has been termed store-operated Ca^{2+} entry (SOCE) (9). In addition to its function in refilling depleted IP_3-sensitive stores, SOCE is important for fine-tuning the transient Ca^{2+} spikes (10) and for inducing Ca^{2+} dependent gene expression (11). Though most extensively studied in non-excitable cells, SOCE has also been described in excitable cells. Despite intensive investigations, neither the proteins that comprise these store-operated Ca^{2+} channels (SOCC), nor the molecular mechanisms underlying activation and gating of these Ca^{2+} channels, have been established. Molecular cloning and functional expression suggest that SOCE is mediated by proteins homologous to the *Drosophila* transient receptor potential (TRP), a Ca^{2+}-permeable non-selective cation channel. Mammalian homologues of TRPs are one of the largest groups of cation channels with diverse functions, biophysical properties, and modes of activation (12). SOCE activation might involve docking or fusion of SOCC containing secretory vesicles with plasma membrane, direct conformational coupling of IP_3 receptors with SOCCs, or the generation and release of a diffusible messenger from the ER upon depletion (13). Recent work has identified the ER membrane-spanning STIM1 (stromal interaction molecule) as the putative ER luminal Ca^{2+} sensor that couples store depletion to SOCE activation (14). STIM1 functionally interacts with CRACM1 (also known as Orai1), a plasma membrane component required for SOCE activity suggesting that the latter may represent the SOCC itself or a regulatory subunit of the SOCC complex (15).

Recent studies have provided evidence that mitochondria can rapidly sequester Ca^{2+} following its influx through SOCC and may modulate SOCE by acting as a local buffer for Ca^{2+} (16–19). Mitochondria are known to play key roles in the regulation of cellular Ca^{2+} dynamics in physiological settings such as excitation-contraction coupling and neurotransmitter release, as well as in pathological states. Because mitochondria play major roles in energy metabolism and production of ROS, perturbations of mitochondrial ATP and ROS production can affect cellular Ca^{2+} homeostasis, and vice versa (20, 21). Changes in mitochondrial transmembrane potential can affect the ability of the mitochondria to take up Ca^{2+}, which is important for the regulation of intramitochondrial oxidative metabolism (22). Although UCPs have been shown to modulate mitochondrial membrane potential, and ROS and ATP production, little is known about their contribution to neuronal Ca^{2+} homeostasis. To elucidate whether UCPs may function in Ca^{2+} homeostasis, we measured mitochondrial Ca^{2+} sequestration following IP_3-dependent and independent agonist-induced store depletion and the SOCE pathway in PC12 cells expressing or lacking human UCP4 (hUCP4). These data demonstrate that hUCP4 regulates mitochondrial Ca^{2+} sequestration and Ca^{2+} entry but not release from intracellular stores. Furthermore, expression of hUCP4 decreases the magnitude of sustained elevation in $[Ca^{2+}]_i$ after cellular Ca^{2+} depletion, inhibits mitochondrial Ca^{2+} overload and oxidative stress, and prevents cell death.

EXPERIMENTAL PROCEDURES

Cell Cultures and Transfection—Clones of PC12 cells stably overexpressing full-length hUCP4 were generated using methods similar to those described previously (23). The recombinant plasmid encoding full-length hUCP4 (pcDNA-hUCP4) was kindly provided by G. Pan (Genentech). PC12 cells were subcultured into 6-well plates coated with polyethyleneimine and grown to 80% confluency in culture medium consisting of Dulbecco's modified Eagle's medium supplemented with 10% horse and 5% fetal bovine serum. Transfection was performed using 1 μg of purified plasmid DNA and 10 μl of Lipofectamine reagent (Invitrogen). Stable transfectants were obtained after selection for growth in the presence of Geneticin (500 mg/liter). Several clones of cells expressing moderate levels of UCP4 protein were selected and maintained in the presence of Geneticin (200 mg/liter). For experiments, PC12 cells were plated onto glass coverslips and used between 18 and 48 h after plating. Transient transfection with the expression plasmid encoding the mitochondrially targeted fluorescent marker DsRed (mtDsRed) cloned into pcDNA3 (Invitrogen), was performed using Lipofectamine.

Experimental Treatments—Undifferentiated PC12 cells were treated with thapsigargin (TG), *N*-acetyl-D-sphingosine (C_2-ceramide), C_2-dihydroceramide, and aristolochic acid (Aris, Alexis Biochemicals). All reagents except when noted were from Sigma. When Me_2SO or ethanol was used as the solvent, their final concentration did not exceed 0.1%. At the end of each treatment, cultures were processed for immunoblotting, and for evaluating the extent of cell death.

Targeting 21-mer siRNA duplexes with a two-base overhang corresponding to the Gadd153 coding regions nucleotides 270–291 ($siRNA_{Gadd153}$, GenBank™ accession number NM_024134) were synthesized using the Silencer siRNA Construction Kit (Ambion, Austin, TX). Briefly, sense primers and corresponding antisense primers were mixed, heated to 95 °C for 5 min, and then allowed to cool to 25 °C at a rate of 1 °C/min as previously described (23). Non-silencing control siRNA ($siRNA_{CTRL}$) duplexes were synthesized using scrambled sequences. A GenBank™ search revealed no other known genes exhibiting sequence homology to these selected target sequences. To test the silencing effect of siRNAs on the induction of Gadd153, normal PC12 cells were transfected with the targeting or control siRNA duplexes (100 nM) for 14 h prior to exposure to TG. The effects of siRNA on vulnerability to TG-induced death were evaluated after transfection of siRNAs.

RNA Isolation and RT-PCR—Total RNA was extracted from neuronal cultures using TRIzol reagent (Invitrogen). 2 μg of RNA was used for synthesis of cDNA using random primers and a first strand synthesis kit (Invitrogen). 200 ng of the cDNA was used in the PCR reaction using the following pairs of primers: hUCP4: 5′-CTGGACTGGTAGCTTCTATTCTGGG-3′ (forward) and 5′-TTAAAATGGACTGACTCCACTCATC-3′ (reverse); rUCP2: 5′-GGCTGGCGGTGGTCGGAGAT-3′ (forward) and 5′-CAACGGGGGAGGCAATGACG-3′ (reverse); rUCP4: 5′-TCCTTCCCTGACCTCTCTTG-3′ (forward) and 5′-TCTCCAAAGCACTACAAAGTC-3′ (reverse); TRPC1: 5′-ACAGATGTTACAAGATTTTGGG-3′ (forward) and 5′-AACTTCCATTCTTTATCC-

TCATG-3′ (reverse); TRPC4: 5′-GCCTACACCTTTCAATGTCATCCC-3′ (forward) and 5′-CTTAGGTTATGTCTCTCGGAGGC-3′ (reverse); TRPC5: 5′-CTATGAGACCAGAGCTATTGATG-3′ (forward) and 5′-CTACCAGGGAGATGACGTTGTATG-3′ (reverse); TRPC6: 5′-GTGCCAAGTCCAAAGTCCCTGC-3′ (forward) and 5′-CTGGGCCTGCAGTACGTATC-3′ (reverse); and glyceraldehyde-3-phosphate dehydrogenase: 5′-ACCACAGTCCATGCCATCAC-3′ (forward) and 5′-TTGTAACCAACTGGGACGATATG-3′ (reverse). The optimized PCR conditions were 2 min at 94 °C, 35 cycles of 94 °C for 30 s, 58 °C for 30 s, 72 °C for 45 s, and 10 min at 72 °C. The PCR products were separated on a 1.5% agarose gel, stained with ethidium bromide, and visualized using a Fuji 3000 PhosphorImager.

Immunoblot Analysis—Methods for protein quantification, electrophoretic separation, and transfer to nitrocellulose membranes were described previously (23). Membranes were incubated in blocking solution (5% milk in Tween Tris-buffered saline) overnight at 4 °C followed by a 1-h incubation in primary antibody diluted in blocking solution at room temperature. Membranes were then incubated for 1 h in secondary antibody conjugated to horseradish peroxidase (Vector Laboratories), and bands were visualized using a chemiluminescence detection kit (ECL, Amersham Biosciences). The primary antibodies included rabbit polyclonal antibodies against hUCP4 (Alpha Diagnostic), SERCA2 (Dr. J. Lytton, University of Calgary), calreticulin (Sigma), TRPCs 1, 4, and 5 (Alomone Laboratories), and STIM1 (Dr. J. Roos, TorreyPines Therapeutics); mouse monoclonal antibodies against actin (Sigma), HSP60 (Signal Transduction), cytochrome *c* oxidase 1 (Molecular Probes), Bcl-2 (StressGen), Grp78 (StressGen), KDEL (StressGen), and Gadd153 (Santa Cruz Biotechnology). Membranes were stripped and re-probed with the actin antibody to verify and normalize protein loading (50 μg of total protein, unless stated otherwise). To determine the presence of the mitochondria in subcellular fractions, membranes were re-probed with the cytochrome *c* oxidase 1 antibody.

Quantification of Cell Survival—Cell viability was assessed by the trypan blue exclusion method as described previously (23).

Confocal Laser Microscopy—Mitochondria organization was visualized in cells transiently transfected with mitochondrially targeted fluorescent marker DsRed as described previously (23). Cells were illuminated 24 h post-transfection at 575 nm, and emission was monitored at 528–633 nm.

Measurement of Mitochondrial Membrane Potential and ROS Formation—Mitochondrial membrane potential was determined in cultured cells using cell permeant probe tetramethylrhodamine (TMRE, Molecular Probes) or MitoTracker Red CMXRos (Molecular Probes) as described previously (23). Accumulation of TMRE in mitochondria is dependent on the polarization state of the mitochondrial membrane. Each culture dish was incubated with 50 nM TMRE for 20 min at 37 °C and then rinsed with Locke's buffer (in mM: 154 NaCl, 5.6 KCl, 2.3 $CaCl_2$, 1.0 $MgCl_2$, 3.6 $NaHCO_3$, 5 HEPES, and 10 D-glucose, pH 7.2). Cells were imaged using a confocal laser scanning microscope coupled to an inverted microscope; cells were located under bright-field optics and then scanned once with the laser (488 nm excitation and 529 nm emission). Data were expressed as the ratio of the change in fluorescence (dF/F_o) after each treatment.

To assess formation of cellular ROS, cells were incubated for 30 min in the presence of the fluorescent probe dihydrorhodamine 123 (10 μM DHR, Molecular Probes) or 2,7-dichlorodihydrofluorescein diacetate (10 μM DCF, Molecular Probes). DHR localizes mainly in the mitochondria and is oxidized by several ROS, most notably hydrogen peroxide and peroxynitrite, to the positively charged rhodamine 123 derivative. The mitochondrial pixel intensity for 100 individual cells in five different fields per culture in triplicate was averaged, and background fluorescence was subtracted.

Measurement of Cytoplasmic and Intra-mitochondrial Free Ca^{2+} Concentrations—Fluorescence ratio imaging of the Ca^{2+} indicator dye fura-2 acetylmethyl ester (fura-2/AM, Molecular Probes) was used to quantify free intracellular Ca^{2+} concentration ($[Ca^{2+}]_i$) using methods detailed previously (23). Cells were incubated for 15 min in the presence of 2 μM fura-2/AM at 37 °C, washed twice with Locke's buffer, and allowed to incubate for 10 min before imaging. Cells were imaged using the Zeiss Attofluor system with a 40× oil immersion objective lens. The ratio of the fluorescence emission using two different excitation wavelengths (340 and 380 mm) was used to determine $[Ca^{2+}]_i$. In some experiments Ca^{2+} was omitted from the Locke's buffer without (Ca^{2+}-deficient buffer) or with 100 μM EGTA (Ca^{2+}-free buffer). Where indicated, the Locke's buffer was supplemented with an appropriate amount of $CaCl_2$. SOCE was induced by stimulation with TG or bradykinin (BK). SKF-96365 (Tocris) was used to block Ca^{2+} entry, and the ionophore 4-bromo-A23187 (Calbiochem) was added to induce rapid extrusion of Ca^{2+} from intracellular stores out of the cell. Ru360 (Calbiochem), a membrane-permeable analogue of ruthenium red, was used to prevent mitochondrial Ca^{2+} uptake.

Cells treated with 2 μM carbonyl cyanide *m*-chlorophenylhydrazone (CCCP, Sigma) were preincubated with 1 μM oligomycin to inhibit mitochondrial ATPase and thereby to protect the cells from ATP depletion under conditions when membrane potential was collapsed by CCCP. Mitochondrial free Ca^{2+} levels were quantified in cells loaded with the cell-permeant acetoxymethyl ester (AM) form of the fluorescence probe dihydrorhodamine-2 (Rhod-2, Molecular Probes). Cells were incubated with 2 μM Rhod-2/AM for 45 min at 37 °C and were then washed with Locke's buffer. Fluorescence images of randomly chosen fields with 30–40 cells in each field were acquired (excitation, 543 nm; emission, 576 nm) using a confocal microscope. The laser beam intensity and photodetector sensitivity were held constant across cultures to allow quantitative comparisons of relative fluorescence intensity of cells between treatment groups. The illumination intensity was kept to a minimum to prevent artifactual mitochondrial Ca^{2+} loading. Control experiments were performed using CCCP with oligomycin. Fluorescence (*F*) was quantified over the whole surface of each cell body (nucleus excluded) in the selected fields using software provided by the manufacturer (Zeiss), and the mean intensity per cell was then calculated. Values were

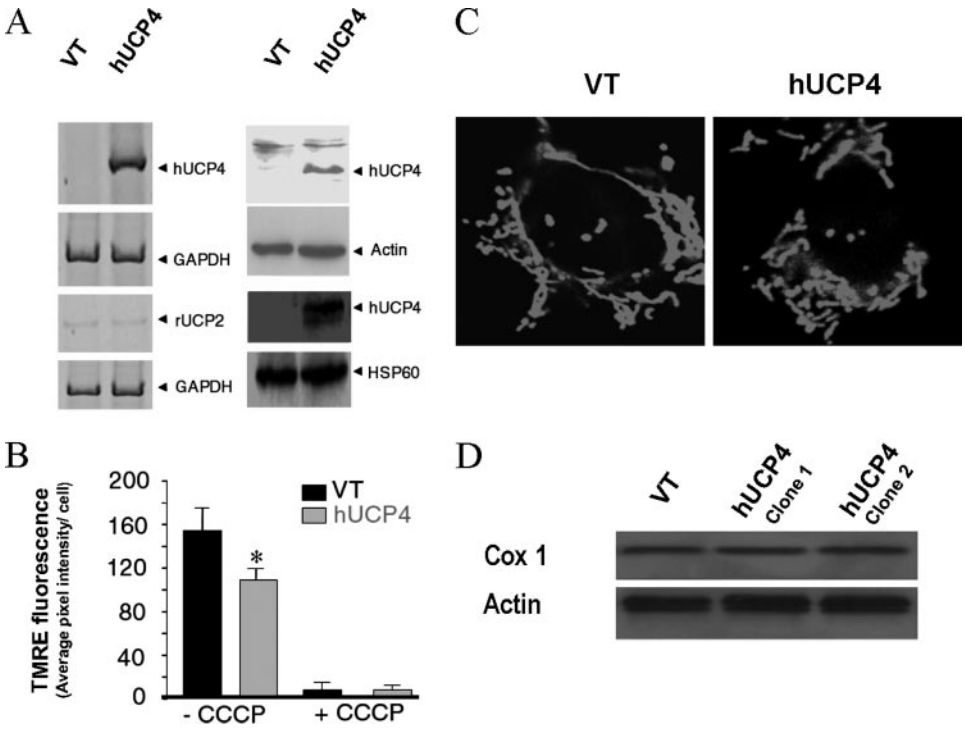

FIGURE 1. **hUCP4 expression reduces mitochondrial membrane potential without affecting mitochondrial mass or subcellular distribution.** *A*, the *panel* at the *left* shows the results of semi-quantitative RT-PCR analysis of human UCP4 (*hUCP4*) and rat UCP2 (*rUCP2*) mRNAs in PC12 cell clones transfected with empty vector (*VT*) or hUCP4 vector. The *panel* at the *right* shows the results of immunoblot analysis of hUCP4 protein levels in whole cell lysates (*upper blot*) and in isolated mitochondria (*third blot*); blots were reprobed with antibodies against either actin or heat shock protein 60 (*HSP60*, a mitochondrial protein) to confirm equal levels of protein loading among samples. *B*, TMRE was used to measure mitochondrial membrane potential in vector-transfected control cells (*VT*) and hUCP4-expressing cells. Values are the mean ± S.D. of determinations made in four separate cultures (40–60 cells assessed/culture); *, $p < 0.05$. *C*, confocal images showing mitochondria-associated fluorescence in VT and hUCP4 cells 36 h after transfection with the mtDsRed vector (see "Experimental Procedures"). *D*, immunoblots showing comparable levels of mitochondrial COX-1 protein levels in VT and in two clones of hUCP4-expressing cells.

expressed as the ratio of the change in fluorescence (dF/F_o) after each time point after treatment.

Loading and Cleavage of Bis-BODIPY-FL-C11-PC—Preparation of bis-BODIPY-FL-C11-PC (a synthetic phospholipid containing fluorescein in position 2 that is dequenched upon cleavage) in liposomes was performed according to the manufacturer's specification (Molecular Probes). PC12 cells were loaded with bis-BODIPY-FL-C11-PC for 30 min, rinsed twice and incubated in Dulbecco's modified Eagle's medium for another 30 min prior to exposure to TG. Fluorescence images were acquired with the confocal imaging system. The data values are corrected for background fluorescence.

Statistical Comparisons—Comparisons between cell types and treatment groups were made using analysis of variance with Scheffe post-hoc test for pairwise comparisons.

RESULTS

hUCP4 Localizes to Mitochondria and Alters Mitochondrial Membrane Potential—Expression of hUCP4 in stably transfected PC12 cells was verified by RT-PCR and by immunoblot analysis using a UCP4 antibody. hUCP4 mRNA was detected in cells stably transfected with vector containing hUCP4 but not with the empty vector (Fig. 1*A*, *left panel*). A 32-kDa immunoreactive band, the predicted size of UCP4, was present in whole cell lysates and in the mitochondrial fraction of hUCP4 but not vector-transfected (VT) cells (Fig. 1*A*, *right panel*). A weak immunoreactive band with a slightly higher molecular weight was present in VT cells (indicated by the *asterisk*). Because we have been unable to detect endogenous rat UCP4 mRNA in PC12 cells (data not shown), the immunoreactive band is likely UCP2, which is known to be expressed in PC12 cells (24). Expression of hUCP4 in PC12 cells did not cause changes in the level of UCP2 mRNA (Fig. 1*A*, *left panel*).

To assess the effects of hUCP4 expression on mitochondrial membrane potential, we loaded cells with low concentrations of the fluorescence probe TMRE. Fluorescence images were acquired using a confocal microscope and quantified (25). hUCP4 cells exhibited reduced TMRE fluorescence compared with control cells demonstrating that expression of hUCP4 reduces steady-state mitochondrial membrane potential (Fig. 1*B*), which was sensitive to complete dissipation of the hydrogen ion gradient induce by the cell-permeant protonophore CCCP. Addition of oligomycin did not depolarize nor restore the difference in mitochondrial membrane potential suggesting that the mitochondrial membrane potential in hUCP4 cells was not maintained by the mitochondrial ATP synthase functioning in reverse mode and consuming ATP produced by glycolysis. This decrease in mitochondrial membrane potential led to a slight but significant increase in oxygen consumption suggesting the functional uncoupling activity is due to the expressed UCP4 in PC12 (26). Furthermore, we found that intracellular ATP content was maintained suggesting no disruption in cellular energetics in hUCP4-expressing cells (26). The staining pattern of the mitochondrial targeted fluorescence marker DsREd was similar in vector-transfected and hUCP4-expressing cells (Fig. 1*C*), indicating that hUCP4 expression did not grossly affect mitochondrial distribution (Fig. 1*C*). Levels of cytochrome oxidase (cytochrome *c* oxidase 1), a mitochondrial protein, remain unchanged (Fig. 1*D*), indicating that hUCP4 did not induce mitochondrial proliferation as has been reported in brain cells of UCP2 transgenic mice (24).

hUCP4 Expression Reduces Mitochondrial Ca^{2+} Sequestration—To evaluate how hUCP4 affects mitochondrial Ca^{2+} homeostasis, we first measured the cytoplasmic free Ca^{2+} concentrations in VT and hUCP4-transfected cells following stimulation with the IP_3 agonist bradykinin in the absence of extracellular Ca^{2+}. The resting $[Ca^{2+}]_i$ level was similar in VT and

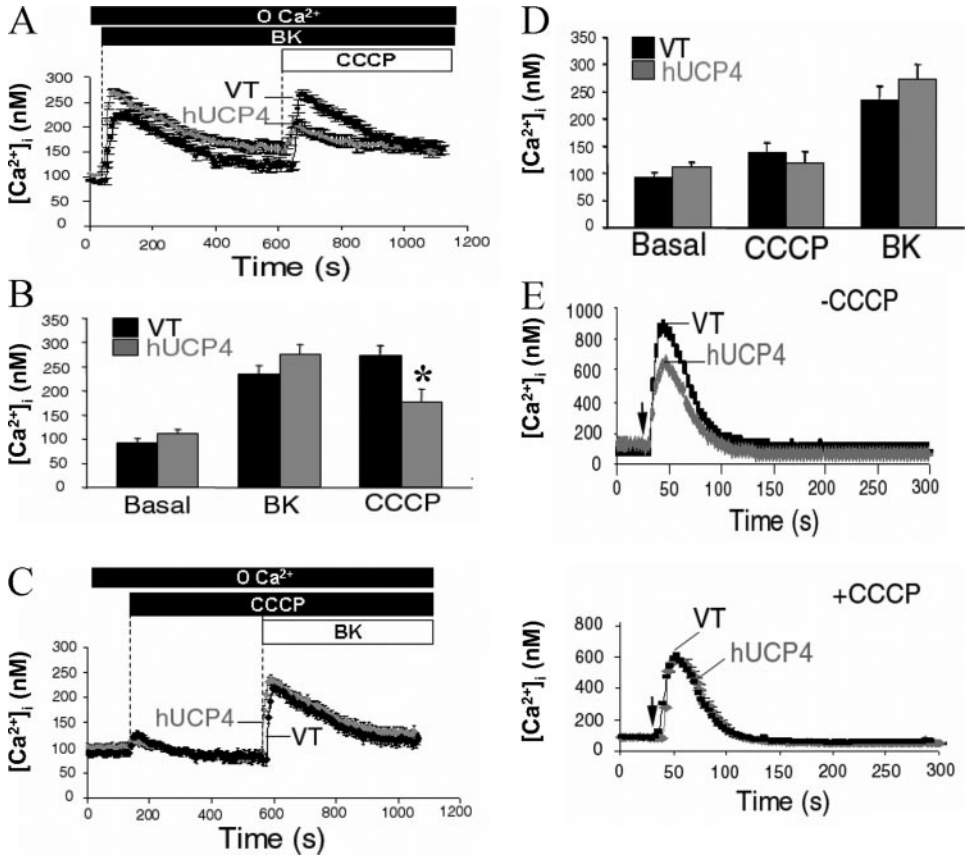

FIGURE 2. **hUCP4 reduces mitochondrial Ca^{2+} sequestration following Ca^{2+} release from internal stores.** *A*, recordings showing the mean $[Ca^{2+}]_i$ before and after sequential additions of 10 μM bradykinin (*BK*) and 2 μM CCCP (plus 1.0 μM oligomycin to prevent ATP depletion) to VT and hUCP4-expressing PC12 cells incubated in Ca^{2+} free medium. Cells were loaded with fura-2, and $[Ca^{2+}]_i$ was recorded as described under "Experimental Procedures." *B*, values of the basal $[Ca^{2+}]_i$ and the peak $[Ca^{2+}]_i$ after exposure to BK and CCCP in VT and hUCP4-tansfected cells. Values are the mean ± S.D. of determinations made in four separate cultures (40–60 cells assessed/culture), *, $p < 0.01$ compared with the value for CCCP-treated VT cells. *C*, recordings showing the mean $[Ca^{2+}]_i$ before and after sequential additions of 2 μM CCCP and 10 μM BK to fura-2-loaded VT and hUCP4-expressing PC12 cells incubated in Ca^{2+}-free medium. *D*, values of the basal $[Ca^{2+}]_i$ and the peak $[Ca^{2+}]_i$ after exposure to CCCP and BK in VT and hUCP4-tansfected cells. Values are the mean ± S.D. of determinations made in four separate cultures (40–60 cells assessed/culture). *E*, recordings showing 4-bromo-A23187-induced $[Ca^{2+}]_i$ elevation in VT and hUCP4-transfected cells that had been preincubated in the absence (*top graph*) or presence (*bottom graph*) of CCCP. The *arrow* indicates time of addition of the Ca^{2+} ionophore (1 μM).

hUCP4-expressing cells (Fig. 2, *A* and *B*). Compared with VT cells, the transient bradykinin-induced $[Ca^{2+}]_i$ increase in Ca^{2+}-free buffer was higher in hUCP4 cells but did not reach statistically significance (237 ± 21 and 261 ± 24 nM, respectively, Fig. 2, *A* and *B*). Addition of CCCP to collapse the mitochondrial membrane potential caused a transient rise in $[Ca^{2+}]_i$ that was significantly lower in hUCP4-transfected cells compared with VT cells (208 ± 21 and 272 ± 25 nM, respectively, Fig. 2, *A* and *B*). Similar results were obtained when cells were treated with TG (an inhibitor of the sarco(endo)plasmic reticulum Ca^{2+} ATPases) instead of BK (data not shown). Next, we determined whether hUCP4 expression affects ER Ca^{2+} store content or release. In the presence of CCCP, the BK-induced $[Ca^{2+}]_i$ transient was comparable in hUCP4 and VT cells (241 ± 20 and 231 ± 21 nM, respectively, Fig. 2, *C* and *D*), suggesting that hUCP4 does not affect the kinetics of agonist-induced Ca^{2+} release. The CCCP-induced $[Ca^{2+}]_i$ transient was similar in VT and hUCP4 cells (121 ± 9 and 132 ± 11 nM, respectively) indicating that hUCP4 expression did not significantly alter the steady-state $[Ca^{2+}]_m$. We also exposed cells pre-incubated with or without CCCP to the Ca^{2+} ionophore 4-bromo-A23187 (1 μM) in Ca^{2+}-deficient buffer to assess whether hUCP4 expression may alter the ER Ca^{2+} store. The ionophore caused rapid extrusion of Ca^{2+} from intracellular stores out of the cell. In the absence of CCCP, the ionophore-releasable Ca^{2+} pool was significantly lower in hUCP4-transfected cells compared with VT cells (Fig. 2*E*, *upper panel*; 602 ± 34 nM and 824 ± 23 nM, respectively). On the other hand, the elevation of $[Ca^{2+}]_i$ induced by the ionophore when mitochondrial Ca^{2+} uptake was inhibited was not different in hUCP4-transfected cells compared with VT cells (Fig. 2*E*, *lower panel*; 592 ± 34 nM and 625 ± 23 nM, respectively). These data suggest that hUCP4 expression has little or no effect on the ER Ca^{2+} store content and release and that mitochondria in cells expressing hUCP4 have a reduced capacity to store Ca^{2+} that has been released from the ER.

Evidence That hUCP4 Attenuates the Store-operated Ca^{2+} Entry Pathway—Depletion of Ca^{2+} stores by either IP_3-dependent or IP_3-independent pathways results in activation of SOCE (9). Recent studies indicate that mitochondrial Ca^{2+} buffering is essential for SOCE and that inhibition of mitochondrial Ca^{2+} uptake, either by mitochondrial depolarization or by inhibition of the mitochondrial Ca^{2+} uniporter, impairs SOCE (16–19). Because the data above suggested that UCP4 may affect mitochondrial Ca^{2+} regulation, we investigated the mechanism by which UCP4 affects the SOCE pathway. To fully activate SOCE, we emptied intracellular stores with 1 μM TG in the absence of extracellular Ca^{2+} for 10 min. The slow and transient increase in $[Ca^{2+}]_i$ evoked by TG due to the leak of Ca^{2+} from the stores was not significantly different in VT and hUCP4-transfected cells (Fig. 3*A*). Subsequent exposure of cultures to a range of external Ca^{2+} concentrations ($[Ca^{2+}]_e$) resulted in a substantial concentration-dependent increase in $[Ca^{2+}]_i$, which did not return to the basal level but, instead, decreased slowly to a steady-state level of elevated $[Ca^{2+}]_i$. This plateau $[Ca^{2+}]_i$ reflects the balance between Ca^{2+} influx into the cytosol through SOCE, which is gradually reduced by a feedback inhibition by Ca^{2+}, and Ca^{2+} efflux from the cells driven mainly by plasma membrane Ca^{2+} ATPase. Expression of hUCP4 decreased both the peak amplitude and steady-state

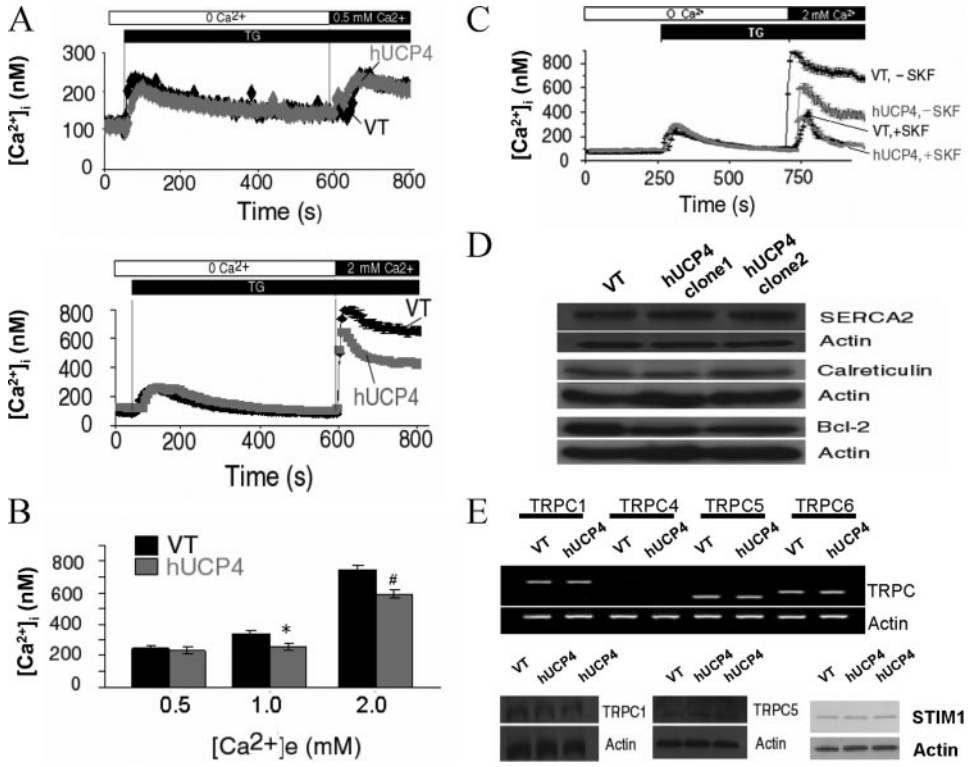

FIGURE 3. **Expression of hUCP4 reduces store-operated Ca^{2+} entry.** *A* and *B*, store-operated Ca^{2+} entry was assessed by depleting Ca^{2+} stores with 1 μM thapsigargin (*TG*) in Ca^{2+}-free medium for 15 min, followed by exposure of fura-2-loaded cells to medium containing 0.5 or 2.0 mM Ca^{2+} (*upper* and *lower graphs* in *panel A*, respectively) to initiate Ca^{2+} entry. The values in *panel B* are the mean ± S.D. of determinations made in three or four cultures (30–40 cells assessed per culture). *, $p < 0.05$; #, $p < 0.01$. *C*, preincubation of fura-2-loaded VT and hUCP4 cells with 10 μM SKF-96365 (a SOCE blocker) for 5 min markedly attenuates SOCE induced by 1 μM TG. *D*, immunoblot analyses showing protein levels of calreticulin, SERCA2, and Bcl-2 in VT cells and two clones of hUCP4-transfected cells. *E*, RT-PCR analysis (*upper panel*) showing mRNA levels of TRPCs and actin, and immunoblots (*lower panels*) showing protein levels of TRPCs, STIM1, and actin in one or two clones of hUCP4-expressing cells.

level of $[Ca^{2+}]_i$ during the store refilling period when the $[Ca^{2+}]_e$ was increased to 1.0 mM or greater (Fig. 3*B*). Following addition of 2 mM Ca^{2+}, the average rise in $[Ca^{2+}]_i$ level was 762 ± 56 and 553 ± 43 nM in VT and hUCP4-transfected cells, respectively (Fig. 3*B*). A $[Ca^{2+}]_e$ of 2 mM, which represents the physiological level of extracellular calcium, was chosen for all subsequent experiments to better appreciate differences in Ca^{2+} signals.

It is unlikely that hUCP4 interfered with the intensity of the coupling signal transmitted from ER to plasma membrane SOCC, because the initial rate of $[Ca^{2+}]_i$ change was similar in both VT and hUCP4-expressing cells (Fig. 3*A*). To determine whether hUCP4 may interfere with TG-induced depletion of intracellular Ca^{2+} stores, we assessed the ability of BK to release Ca^{2+} following exposure of cells to TG. Addition of 100 μM BK failed to elicit further increase in $[Ca^{2+}]_i$ in either VT or hUCP4-transfected cells (data not shown) suggesting that stores were indeed fully depleted and that the reduction of SOCE in hUCP4 cells could not be attributed to incomplete store depletion. Preincubation of cells with SKF-96365, a widely employed inhibitor of SOCE, strongly inhibited TG-induced Ca^{2+} entry (Fig. 3*C*), suggesting that the rise in $[Ca^{2+}]_i$ is mainly attributed to SOCE. To assess whether hUCP4 may enhance Ca^{2+} extrusion mechanisms, we added EGTA during store refilling to abruptly inhibit Ca^{2+} influx. The rapid decay of the steady state $[Ca^{2+}]_i$ and hence the initial rate of Ca^{2+} clearance, which mostly reflects Ca^{2+} extrusion rate was comparable in VT and hUCP4-transfected cells (data not shown). Taken together, these data support the argument that expression of hUCP4 diminishes mitochondrial Ca^{2+} sequestration and SOCE rather than enhancing Ca^{2+} efflux across plasma membrane.

hUCP4 Does Not Alter Expression of Proteins in the SOCE Pathway—We next determined whether overexpression of hUCP4 affects levels of proteins involved in the SOCE pathway. Steady-state levels of SERCA2 and the ER luminal Ca^{2+} binding/storage protein calreticulin, two ER proteins that regulate ER Ca^{2+} store refilling and, indirectly, SOCE (27) were not significantly different in hUCP4-transfected and VT cells (Fig. 3*D*). Levels of Bcl-2, a protein that has been shown to play a role in ER Ca^{2+} homeostasis (28, 29), were also similar in VT and hUCP4 cells. Because the SOCE response was reduced in hUCP4 cells, we determined whether expression of TRP-related proteins was down-regulated in hUCP4 cells. Previous studies showed that induction of differentiation and chronic hypoxia increased expression of several TRPC proteins (a subfamily of TRPs), which was accompanied by an increase in SOCE activity (30). PC12 cells express most of the six TRPC (TRP 1–6) members (31). Despite their similarity in amino acid sequence, members of the TRPC subfamily have different modes of activation (12). Some TRPC proteins form Ca^{2+}-permeable cation channels that do not appear to be store-operated; they do not respond to treatment with TG, the most selective pharmacological tool for activating SOCE. Because store-depletion-insensitive TRPCs may heteromultimerize with store-depletion-sensitive TRPCs to form functional SOCC (12), we analyzed the expression of TRPs 1, 4, 5, and 6 in VT and hUCP4-transfected cells. TRPC4 mRNA was not detected in VT or hUCP4 cells (Fig. 3*E*). Steady-state levels of TRPCs 1, 5, and 6 mRNA measured by RT-PCR were not affected by hUCP4 expression (Fig. 3*E*); similarly, levels of TRPC proteins 1 and 5 were not different in VT and hUCP4 cells. Moreover, the protein level of STIM1, the putative ER calcium sensor (14, 15), was not different in VT and hUCP4 cells. Thus, it is unlikely that altered expression of TRPCs or STIM1 contributed to the observed effect of hUCP4 in reducing SOCE.

hUCP4 Regulates SOCE at the Level of Mitochondrial Ca^{2+} Sequestration—To determine whether mitochondrial Ca^{2+} uptake is essential for maintenance of SOCE, we induced com-

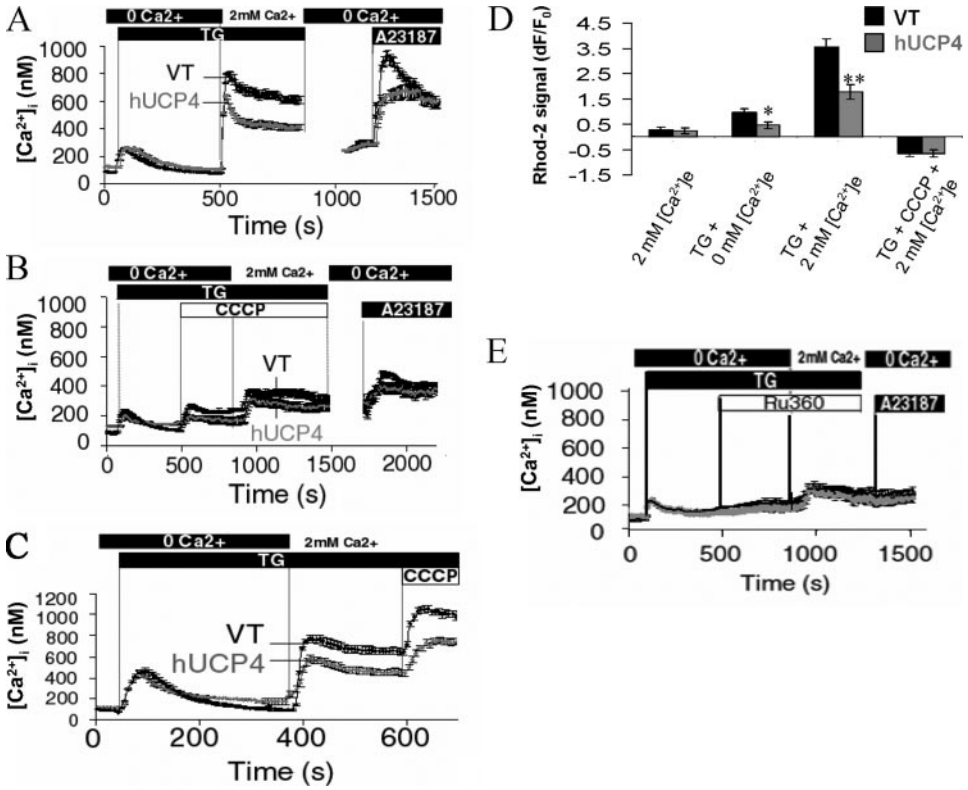

FIGURE 4. **hUCP4 reduces mitochondrial Ca^{2+} loading during store depletion-induced SOCE.** *A*, recordings showing the mean $[Ca^{2+}]_i$ before and after exposure of fura-2-loaded VT and hUCP4 cells to the indicated treatments (thapsigargin (*TG*), 1 μM; 4-bromo-A23187, 10 μM). *B* and *C*, recordings of $[Ca^{2+}]_i$ in fura-2-loaded VT and hUCP4 cells exposed to the indicated treatments (*TG*, 1 μM; 4-bromo-A23187, 1 μM; CCCP, 2 μM plus 1.0 μM oligomycin). *D*, Rhod-2 fluorescence in VT and hUCP4 cells exposed to the indicated treatments; measurements were made 2 min after addition of vehicle or TG alone, or in combination with 2 mM Ca^{2+} to induce SOCE. Shown are the ratios of the change in fluorescence signal (relative to vehicle alone) and S.D. of measurements made in three or four cultures (30–40 cells assessed per culture). *, $p < 0.05$ and **, $p < 0.01$ compared with corresponding values of VT cells. *E*, recordings showing the mean $[Ca^{2+}]_i$ before and after exposure of fura-2-loaded VT and hUCP4 cells to the indicated treatments (TG, 1 μM; Ru360, 10 μM; 4-bromo-A23187, 10 μM).

plete store depletion with TG in Ca^{2+}-free medium and assessed the amount of releasable Ca^{2+} from mitochondria ($[Ca^{2+}]_m$) in TG-treated cells during re-application of 2 mM Ca^{2+}. Consistent with the results above (Fig. 3, *A* and *B*), the magnitude of the $[Ca^{2+}]_i$ rise and the average plateau Ca^{2+} were significantly lower in hUCP4-transfected cells during Ca^{2+} re-application (Fig. 4*A*). To terminate loading, we applied Ca^{2+}-free buffer for another 150 s. Subsequent addition of 4-bromo-A23187 released the Ca^{2+} sequestered in the TG-insensitive mitochondrial store, and the amount of released Ca^{2+} was significantly lower in hUCP4-transfected cells than in VT cells (918 ± 36 *versus* 618 ± 24 nM, Fig. 4*A*) indicating that mitochondria of hUCP4-transfected cells take up less Ca^{2+} during store refilling.

Next, we determined whether acute exposure to CCCP in the presence of oligomycin could mimic the inhibitory action of hUCP4 on the SOCE pathway. When CCCP was applied to TG-treated cells 1 min prior to and during the store-refilling period, TG-stimulated SOCE was largely blocked in both VT and hUCP4-transfected cells (388 ± 34 nM and 340 ± 28 nM, respectively, Fig. 4*B*). Subsequent application of 4-bromo-A23187 in Ca^{2+}-deficient buffer released little Ca^{2+} from the TG-insensitive stores in VT and hUCP4-transfected cells. As expected, CCCP applied to TG-treated cells during the store-refilling period caused release of Ca^{2+} sequestered in the TG-insensitive stores, and the magnitude of this release was significantly lower in hUCP4-transfected cells compared with VT cells (719 ± 46 and 1012 ± 56 nM, respectively, Fig. 4*C*). To verify that the TG-insensitive Ca^{2+} stores were mitochondria, we loaded cells with Rhod-2/AM, a Ca^{2+}-sensitive fluorescent indicator commonly used to monitor changes in $[Ca^{2+}]_m$ (32). The magnitude of the increase in Rhod-2 fluorescence signal was significantly greater in VT cells than in hUCP4 cells following the addition of TG in the absence or presence of extracellular Ca^{2+}. CCCP, which prevented uptake of Rhod-2 into the organelle, inhibited the increase in the fluorescence signal in both cell types, further confirming that the TG-insensitive store is mitochondria (Fig. 4*D*). To further demonstrate that Ca^{2+} uptake by mitochondria is required to sustain SOCE, we used Ru360, a membrane-permeable analogue of ruthenium red that prevents mitochondrial Ca^{2+} uptake by directly inhibiting the Ca^{2+} uniporter without interfering with the mitochondrial membrane potential (33). Treatment with 10 μM Ru360 significantly reduced SOCE in VT cells to an extent comparable to that in hUCP cells (258 ± 19 and 247 ± 13 nM, Fig. 4*E*). As expected, the amount of Ca^{2+} released from the TG-insensitive stores was reduced in Ru360-treated VT and hUCP4 cells upon application of 4-bromo-A23187. Collectively, our data suggest that expression of hUCP4 attenuates the ability of the mitochondria to sequester cytosolic Ca^{2+} and to sustain SOCE (16–19).

hUCP4 Attenuates Store Depletion-induced Cell Death—To determine whether cells expressing hUCP4 are more resistant to death induced by TG, we measured viabilities of VT and hUCP4 cells exposed to TG for various time periods. Compared with VT cells, hUCP4 cells were significantly more resistant to death induced by TG. When exposed to TG for 24 h in medium containing 2 mM Ca^{2+}, 28% of the hUCP4-expressing cells were dead compared with 50% of VT cells (Fig. 5*A*). Decreasing the $[Ca^{2+}]_e$ to 0.5 mM protected VT cells against TG-induced death, effectively eliminating the protective effect of hUCP4 (Fig. 5*A*). These findings suggested that hUCP4 protects cells by reducing SOCE. Consistent with this conclusion we found that the L-type Ca^{2+} channel blocker nimodipine (1 μM) had no significant effect on TG-induced death (data not shown). Because exposure of PC12 cells to SKF-96365 or Ca^{2+}-free medium resulted in cell death within 6–12 h (data not shown),

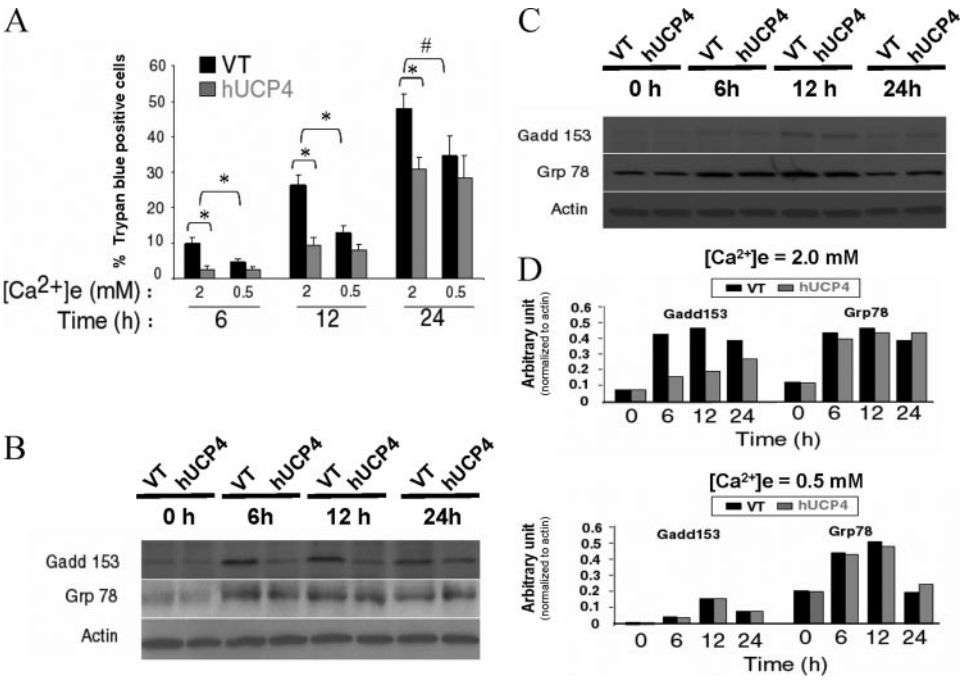

FIGURE 5. **hUCP4 expression protects cells against thapsigargin-induced death.** *A*, cultures of vector-transfected (*VT*) and hUCP4-expressing cells were exposed to thapsigargin (*TG*; 0.5 μM) in medium containing 2.0 and 0.5 mM Ca^{2+} ($[Ca^{2+}]_e$). At the indicated time points viability was assessed by the trypan blue exclusion method. Values are expressed as the percentage of cells that were trypan blue-positive; *bars* represent the mean ± S.D. of determinations made in four separate cultures (100–150 cells assessed/culture); *, $p < 0.01$; #, $p < 0.05$. Comparable results were obtained in additional experiments utilizing a different PC12 clone expressing hUCP4. *B* and *C*, basal and TG-induced levels of the ER stress proteins, growth-arrest DNA damage-inducible (*Gadd*) 153 protein and glucose-regulated protein (*Grp*) 78. Whereas the TG-induced increase in GRP protein levels were comparable, the increase in Gadd153 protein was markedly lower in hUCP4-expressing cells compared with that of VT cells incubated in medium containing 2 mM (*B*) but not 0.5 mM Ca^{2+} (*C*). Blots were reprobed with an actin antibody to confirm equal levels of protein loading among samples. *D*, densitometric analyses were performed on the immunoblots obtained from *B* and *C* in two independent studies. The ratio of the signal of Gadd153 and GRP78 in treated cells incubated in 2.0 (*top panel*) and 0.5 (*bottom panel*) mM $[Ca^{2+}]_e$ at each time point as indicated on the *x*-axis and that of actin is shown on the *y*-axis in arbitrary units.

we were unable to determine their effects on TG-induced cell death.

We found that basal and TG-induced levels of the ER chaperone GRP78, an indicator and key component of the ER stress response (34), were similar in VT and hUCP4-expressing cells (Fig. 5, *B* and *D*), indicating that hUCP4 did not protect against TG-induced death by facilitating induction of this ER chaperone. In contrast, protein levels of the growth-arrest DNA damage-inducible protein 153 (Gadd153), a ubiquitously expressed member of the CAAT/enhancer-binding protein family of transcription factors, increased more rapidly in VT compared with hUCP4 cells (Fig. 5, *B* and *D*). Because Gadd153 is highly induced in response to an elevation of $[Ca^{2+}]_i$ (35), its greater increase following TG treatment in VT cells compared with hUCP4 cells is likely due to the greater sustained elevation in Ca^{2+} as the result of SOCE. Reducing $[Ca^{2+}]_e$ to 0.5 mM resulted in not only an attenuation but also a normalization of the TG-induced increase in Gadd153 protein levels in VT and hUCP4-expressing cells (Fig. 5, *C* and *D*). Thus, expression of hUCP4 attenuates cell death by suppressing SOCE and the upregulation of Gadd153.

hUCP4 Protects against Cell Death Induced by Ceramide—Ceramide is generated from membrane sphingomyelin in response to activation of various cytokine receptors and by exposure of cells to oxidative stress; ceramide can induce cell death by activating the SOCE pathway (36). We therefore determined how expression of hUCP4 expression might affect the vulnerability of PC12 cells to ceramide-induced death. VT and hUCP4 PC12 cells were exposed to increasing concentrations of the cell-permeable ceramide analogue C_2-ceramide, and cell viability was determined 12 and 24 h later. Cells expressing hUCP4 were significantly more resistant to C_2-ceramide-induced death compared with VT cells (Fig. 6*A*). The biologically inactive stereoisomer C_2-dihydroceramide (40 μM) had no significant effect on the survival of VT or hUCP4 cells during a 24-h exposure period. To determine whether the protective action of hUCP4 was mediated by its inhibitory role on the SOCE pathway, we measured Ca^{2+} entry in VT and hUCP4 cells after exposure to C_2-ceramide (Fig. 6*B*). C_2-ceramide caused a slow rise in $[Ca^{2+}]_i$ that reached a long-lasting plateau in cells maintained in Ca^{2+}-containing medium; the magnitude of this Ca^{2+} plateau was significantly lower in hUCP4 cells compared with VT cells. In the absence of extracellular Ca^{2+}, the rise in $[Ca^{2+}]_i$ was slower and only transient in both VT and hUCP4 cells (Fig. 6*B*), suggesting that Ca^{2+} entry was required to maintain the Ca^{2+} plateau in cells treated with C_2-ceramide. To determine whether SOCE activity contributed to the increase in $[Ca^{2+}]_m$ in cells treated with C_2-ceramide, we added the Ca^{2+} ionophore 4-bromo-A23187 to cells 10 min after treatment with C_2-ceramide. The rapid $[Ca^{2+}]_i$ rise upon addition of the Ca^{2+} ionophore was markedly reduced in hUCP4-expressing cells (645 ± 34 nM) compared with VT cells (1068 ± 52 nM, $p < 0.01$) (Fig. 6*C*). The relative increase in the resting $[Ca^{2+}]_i$ was also much lower in C_2-ceramide-treated hUCP4-expressing cells compared with VT cells. Reducing $[Ca^{2+}]_e$ to 0.5 mM partially protected VT cells from death induced by C_2-ceramide (data not shown). Immunoblot analysis showed that expression of hUCP4 resulted in an attenuation of the ceramide-induced increase in Gadd153 protein levels compared with VT cells (Fig. 6*D*).

hUCP4 Expression Reduces Oxidative Stress and Preserves Mitochondrial Function—Mitochondria are a major source of intracellular ROS production, and sustained Ca^{2+} entry and mitochondrial Ca^{2+} uptake can increase mitochondrial oxidative metabolism and generation of ROS. Mitochondrial ROS are key inducers of mitochondrial transition pore opening, a process pivotal for cell death in many physiological and pathological settings. To determine whether hUCP4 modulates mitochondrial oxidative stress, we employed DHR, a cell-permeant

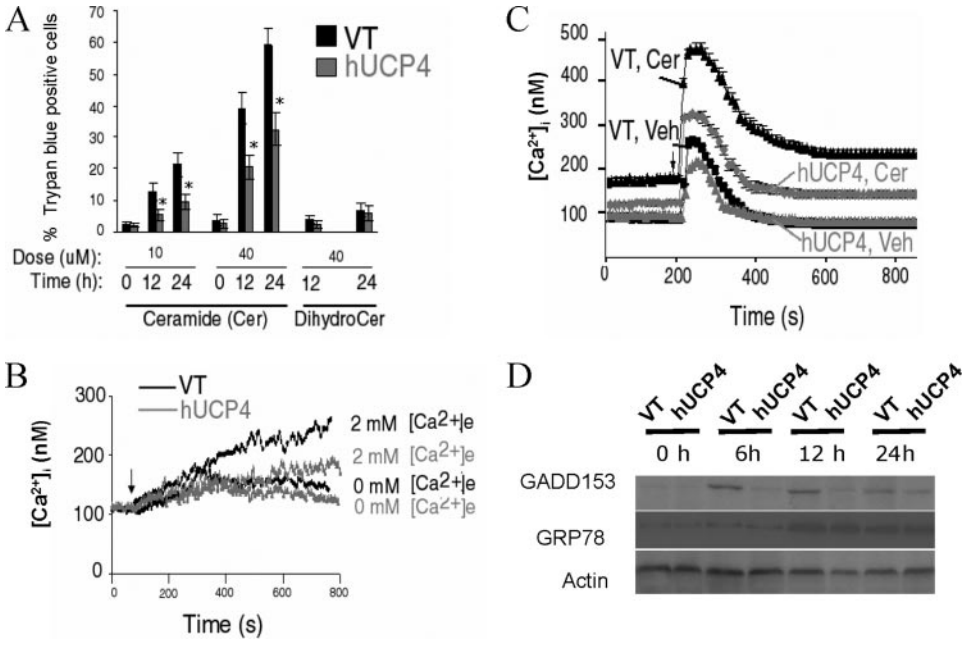

FIGURE 6. **hUCP4 expression protects against cell death induced by ceramide.** *A*, cultures of VT and hUCP4 cells were exposed to different doses of C_2-ceramide (10 and 40 μM) and C_2-dihydroceramide (DHC, 40 μM). At the indicated time points viability was assessed by the trypan blue exclusion method. Values are the mean ± S.D. of determinations made in four separate cultures (100–150 cells assessed/culture); *, $p < 0.01$ compared with the corresponding value for VT cells. *B*, recordings showing the $[Ca^{2+}]_i$ in VT and hUCP4 cells following treatment with C_2-ceramide (20 μM) in the absence or presence of extracellular Ca^{2+}. Cells were loaded with fura-2/AM as described under "Experimental Procedures." The *arrow* indicates time of addition of C_2-ceramide. *C*, recordings showing the $[Ca^{2+}]_i$ in fura-2/AM-loaded VT and hUCP4 cells prior to and during exposure to 4-bromo-A23187 (1 μM) in Ca^{2+}-free buffer. Cells were pretreated with vehicle or 20 μM C_2-ceramide for 10 min prior to exposure to 4-bromo-A23187 (indicated by the *arrow*). *D*, immunoblot showing Gadd153 and GRP78 protein levels in ceramide-treated VT and hUCP4 cells. The blot was reprobed with an actin antibody to confirm equal levels of protein loading among samples. Comparable results were achieved in experiments utilizing an additional PC12 clone expressing hUCP4.

mitochondrial dye, to assess formation of mitochondrial ROS in live cells. Exposure of VT cells to TG caused a rapid increase in DHR fluorescence within 2 h, followed by a sustained peak between 6 and 12 h (Fig. 7*A*). The increase in ROS production was significantly smaller in hUCP4 cells demonstrating that expression of hUCP4 suppresses mitochondrial ROS formation. The increase in DCF fluorescence, which measured cellular peroxide levels, was also reduced in hUCP4 cells at each time point (Fig. 7*A*). We also monitored mitochondrial membrane potential during an 18-h exposure to TG (Fig. 7*B*). The basal membrane potential was greater in VT cells compared with hUCP4 cells. After exposure to TG, the membrane potential in VT cells rose to a peak level at 6 h of exposure and then decreased to a level below the baseline at 18 h. In contrast, the membrane potential in hUCP4 cells rose modestly through 6 h and was maintained at this level through 18 h (Fig. 7*B*). A similar pattern of increases in DHR and TMRE intensities above the level of vehicle-treated cells was obtained in VT and hUCP4 cells exposed to C_2-ceramide (data not shown).

Although mitochondria are prime targets of Ca^{2+}-mediated apoptosis, SOCE could also contribute to Ca^{2+}-dependent events in the cytosol that may indirectly influence mitochondrial function. Recent studies indicate that the extent of Ca^{2+} entry through the SOCE pathway determines the activity of Ca^{2+}-dependent cytosolic phospholipase A2 (cPLA2) (37). Upon activation and translocation to intracellular membranes, cPLA2 generates and releases arachidonic acid from membrane phospholipids (38). To determine whether expression of hUCP4 reduces the generation of arachidonic acid, we loaded cultured cells with the synthetic phospholipid bis-BODIPY-FL-C11-PC, which undergoes dequenching upon hydrolysis by PLA2 to release the labeled phospholipid within the cell. Exposure of bis-BODIPY-FL-C11-PC-loaded cells to TG triggered rapid phospholipid hydrolysis as indicated by an increased fluorescence signal (Fig. 7*C*). The magnitude of the TG-induced lipid hydrolysis was significantly lower, by ~30%, in cells expressing hUCP4 compared with VT cells (Fig. 7*D*). Aristolochic acid, a specific inhibitor of cPLA2, dramatically reduced the fluorescent signal associated with phospholipid release (Fig. 7 D), consistent with the activation of cPLA2 by TG. Incubation of cells in medium lacking Ca^{2+} also largely inhibited TG-induced phospholipid hydrolysis (data not shown). Because arachidonic acid itself, and metabolites generated in the cyclooxygenase or lipoxygenase pathways, can contribute to oxidative stress (39), we determined whether inhibition of cPLA2 activation blocked ROS production. Pretreatment of cells with aristolochic acid partially inhibited TG-induced ROS production (data not shown), suggesting that cPLA2 and its associated metabolic pathways contribute to oxidative stress.

Because oxidative stress can contribute to Gadd153 up-regulation (40–42) and because the magnitude of induction of Gadd153 protein levels was significantly greater in VT compared with hUCP4 cells (Fig. 5, *B* and *D*), we determined whether suppression of Gadd153 function by RNA interference normalized the differential vulnerability of the clones to TG-induced death. The TG-induced increase in Gadd153 protein was attenuated in VT and hUCP4 cells over a course of 14 h in the presence of 100 nM Gadd153 but not scrambled siRNA (Fig. 8*A*). Under these conditions, ER stress-induced expression of two other ER stress proteins, Grp78 and -94, were unaffected by the siRNA treatment. Suppression of endogenous Gadd153 expression partially rescued VT cells from TG-induced death (Fig. 8*B*). In addition, knockdown of Gadd153 function was also more effective compared with aristolochic acid in decreasing the vulnerability of VT cells to TG-induced death (Fig. 8*B*) suggesting that Gadd153 is a critical mediator of store depletion-induced oxidative stress and death.

DISCUSSION

Mitochondria play an important role in intracellular Ca^{2+} dynamics and signaling by sensing microdomains of both Ca^{2+}

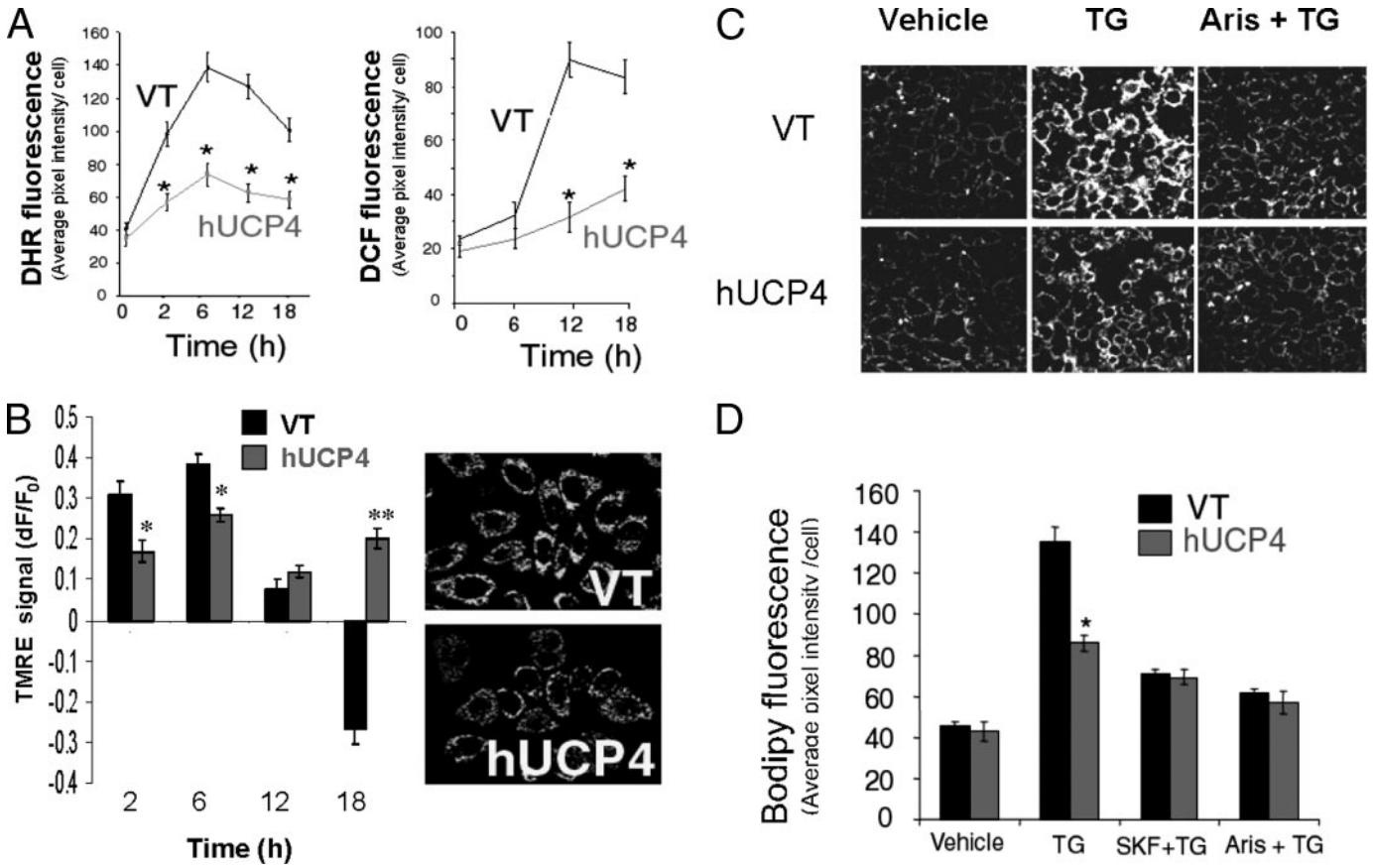

FIGURE 7. **hUCP4 overexpression suppresses ROS generation and stabilizes mitochondrial function.** *A*, hUCP4 expression attenuates TG-induced increases in mitochondrial (DHR fluorescence, *left panel*) and cellular (DCF fluorescence, *right panel*) ROS levels. Values are the average DHR and DCF fluorescence intensity per cell before and after exposure to 0.5 μM TG at the indicated time periods (mean $\pm$ S.D. of determinations made in four to five cultures; 30–40 cells assessed in each culture). *, $p < 0.05$. *B*, hUCP4 attenuates TG-induced mitochondrial hyperpolarization and terminal loss of mitochondrial membrane potential. Shown are the ratios of the changes in TMRE fluorescence signal (relative to untreated cells) and S.D. of determinations made in three to four cultures (20–40 cells assessed in each culture). *, $p < 0.05$ and **, $p < 0.01$, compared with corresponding values of VT cells. Representative images (*right panels*) showing the TMRE fluorescence intensity in VT and hUCP4 cells 6 h after exposure to 0.5 μM TG. *C*, exposure of cells loaded with the synthetic phospholipid bis-BODIPY-FL-C11-PC to TG triggered rapid cPLA2-mediated phospholipid hydrolysis as indicated by the increase in the intracellular fluorescence signal upon dequenching of the released labeled phospholipid. Representative images showing the increase in cell-associated fluorescence in VT and hUCP4 cells 15 min after exposure to TG. *D*, quantification of BODIPY fluorescence in vehicle-treated cells and TG-treated cells before and 15 min after exposure to TG. Values are the mean $\pm$ S.D. of determinations made in three to five cultures. *, $p < 0.01$. Pretreatment with aristolochic acid (*Aris*, a specific inhibitor of cPLA$_2$; 30 μM) or the SOCE blocker SKF-96365 (*SKF*, 10 μM) for 30 min dramatically diminished the increase in fluorescence signal, consistent with the activation of cPLA2 by TG.

release from ER stores and Ca^{2+} influx across the plasma membrane (16–19). It has been shown that within these subcellular microdomains Ca^{2+} is efficiently taken up by mitochondria. The ability of mitochondria to buffer Ca^{2+} locally is essential for gating Ca^{2+}-sensitive plasma membrane channels. Our data suggest that hUCP4 regulates mitochondrial Ca^{2+} homeostasis and sensitivity of neural cells to store depletion-induced death by virtue of its ability to alter the membrane potential-dependent Ca^{2+} buffering capacity of the mitochondria. The effects of hUCP4 on SOCE and cell death were associated with decreased levels of ROS. PC12 cells expressed little or no endogenous UCP4, the level of UCP2 expression was low and unaffected by expression of hUCP4, and hUCP4 had no detectable effects on mitochondrial shape or subcellular distribution. The latter findings suggest that the effects of hUCP4 on store depletion-induced Ca^{2+} entry and cell survival were not secondary to changes in mitochondrial mass.

The key event in the SOCE pathway is intracellular Ca^{2+} store depletion that triggers Ca^{2+} entry upon activation of SOCC in the plasma membrane. The magnitude of the SOCE response is related to the degree to which stores are depleted (9). When exposed to a concentration of TG (1 μM) that induced complete store emptying, PC12 cells expressing hUCP4 exhibited reduced SOCE compared with control VT cells. It is therefore unlikely that the presence of hUCP4 in mitochondria accelerates refilling of the ER Ca^{2+} stores, thereby reducing SOCE. Additional data showed that the decreased SOCE in hUCP4-expressing cells was not attributed to reduced ER Ca^{2+} store content or increased Ca^{2+} extrusion. The steady-state mitochondrial Ca^{2+} levels were not significantly altered in hUCP4 cells at resting state (Fig. 2, *C* and *D*) suggesting that a moderate dissipation of mitochondrial membrane potential has no significant impact on the trans-mitochondrial Ca^{2+} flux responsible for ER refilling (43). Several studies have demonstrated that functional mitochondria are essential for maintenance of SOCE in different cell types (16–19), and dissipation of the mitochondrial membrane potential, which impairs that ability of mitochondria to buffer cytosolic Ca^{2+}, abolishes Ca^{2+} influx through the SOCE pathway after the depletion of intracellular Ca^{2+} stores.

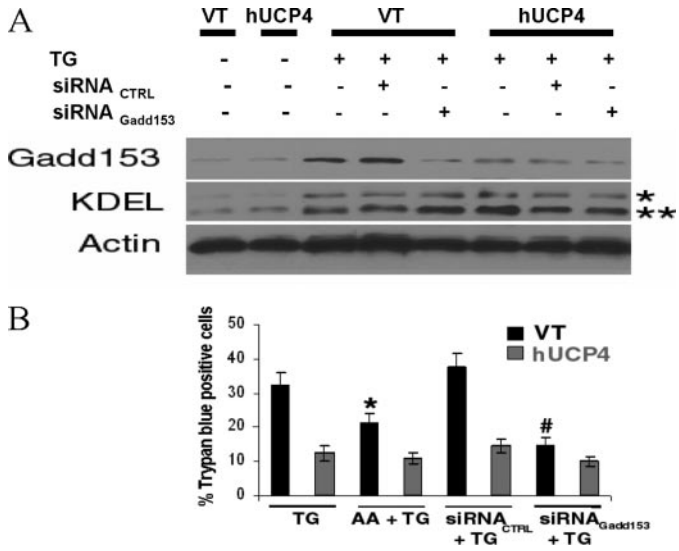

FIGURE 8. **Suppression of Gadd153 induction by RNA interference reduced vulnerability to store depletion-induced apoptosis.** *A*, vector-transfected (*VT*) and hUCP4 cells were pre-treated with 100 nM Gadd153 siRNA ($siRNA_{Gadd153}$) and nonsilencing control siRNA ($siRNA_{CTRL}$) for 14 h prior to exposure to 0.5 μM thapsigargin (*TG*) or vehicle alone (control). Cells were harvested 12 h after TG exposure, and lysates were immunoblotted for detection of endogenous Gadd153 protein, glucose-regulated protein (Grp)78 and Grp94. The TG-induced increase in the latter two stress proteins was detected with an anti-KDEL antibody as indicated by the *single* (Grp94) and *double* (Grp78) *asterisks*. The blot was reprobed with an anti-actin antibody to confirm equal levels of protein loading among samples. *B*, VT and hUCP4 cells were pre-treated either with 100 nM siRNAs ($siRNA_{Gadd153}$ or $siRNA_{CTRL}$) for 14 h or with 30 μM aristolochic acid (*AA*) for 2 h prior to exposure to 0.5 μM TG or to vehicle for 12 h. Cells were fixed for quantitation of cell death. For each treatment condition, the percentage of dead cells in the vehicle-treated group was subtracted from that in the TG-treated group. In the $siRNA_{Gadd153}$-treated groups, the percentage of dead cells was not significantly different. Values are the mean ± S.D. of four separate cultures per group (150–200 cells assessed/culture). *, $p < 0.05$; #, $p < 0.01$, compared with VT cells treated with TG.

The exact mechanism of SOCE modulation by mitochondria is unknown. In addition to buffering Ca^{2+}, mitochondria may release one or more diffusible factors that regulate SOCE activity (13–15, 19). A recent study demonstrated that mitochondrial localization is also an important determinant of SOCE, because relocalization of mitochondria from the subplasma membrane region to perinuclear areas in HeLa cells overexpressing dynamitin caused a significant reduction in SOCE without impacting the ER Ca^{2+} store content (44). Expression of hUCP4 had no detectable effect on mitochondrial numbers or subcellular localization, suggesting that the reduced mitochondrial Ca^{2+} buffering in hUCP4 cells could not be ascribed to a reduction or altered distribution of mitochondria. Furthermore, protein levels of STIM1 (14, 15) and TRPCs, some of which are involved in SOCE (12), were comparable in VT and hUCP4-expressing cells. We therefore propose that the activity of hUCP4 decreases the ability of mitochondria to sequester Ca^{2+} entering the cell, resulting in a fast feedback inhibition of SOCC (16–19). In support for this notion, we found that mitochondrial Ca^{2+} uptake is reduced in hUCP4 cells during agonist-induced ER Ca^{2+} release and Ca^{2+} entry by the SOCE pathway. Similar reductions were seen in hUCP4 cells after store depletion induced by TG and C_2-ceramide. Ca^{2+} uptake is robust in mitochondria situated close to the membranes, which provides a mechanism for rapid sequestration of Ca^{2+} by mitochondria near plasma membrane and ER Ca^{2+} channels. However, massive Ca^{2+} uptake by mitochondria, which can occur during excitotoxic injury and ischemia, can trigger cell death. Recent studies showed that high levels of UCP2 are associated with increased resistance of neurons to excitotoxicity (4), suggesting that a decrease in neuronal mitochondrial membrane potential can suppress Ca^{2+} overload during excitotoxic insults. Consistent with this, Mattiasson *et al.* (5) demonstrated that transgenic mice overexpressing human UCP2 are more resistant to ischemic brain damage compared with nontransgenic control animals, and overexpression of UCP2 in cultured neurons protects them against oxygen/glucose deprivation-induced death. The latter study also showed that mild mitochondrial uncoupling by treatment with 2,4-dinitrophenol prevents the release of pro-apoptotic factors during oxygen-glucose deprivation and reduces neuronal death.

We found that expression of hUCP4 protects against Ca^{2+} store depletion-induced death following exposure to TG and C_2-ceramide. Studies in other cell systems showed that TG toxicity results primarily from mitochondrial Ca^{2+} overload and secondarily from ER stress associated with Ca^{2+} store depletion (45). Expression of hUCP4 blocked mitochondrial ROS formation by reducing the initial hyperpolarization and the subsequent depolarization of the inner mitochondrial membrane potential. Hyperpolarization has been attributed to rapid mitochondrial Ca^{2+} uptake during exposure of neurons to glutamate and oxygen-glucose deprivation (46). With mitochondrial membrane hyperpolarization and extrusions of H^+ ions from the mitochondrial matrix, the cytochromes within the electron transport chain becomes more reduced, which favors generation of ROS (47). The early hyperpolarization coincides with peak generation of ROS (Fig. 7, *A* and *B*). ROS are key inducers of mitochondrial permeability transition pore opening, and this process can trigger release of apoptogenic factors and activation of caspases (48). In addition to the mitochondrially derived ROS, expression of hUCP4 also blocked cPLA2 activation and subsequent oxidative metabolism of phospholipid-derived arachidonic acid via the cyclooxygenase or lipoxygenase pathways, which leads to O_2^- or $OH^\bullet$ production (39). Recent investigations have demonstrated that members of the UCP family can prevent mitochondrial ROS formation, oxidative stress, and the terminal loss of the mitochondrial membrane potential. Using gene knock-out models and *in vitro* systems, several groups demonstrated that UCP2 decreases cellular oxidative damage through a reduction in mitochondrial ROS production (49, 50). The generation of ROS has been clearly established as a contributor to several neurodegenerative diseases and may underlie cellular changes seen in aging. Interestingly, targeted expression of UCP2 to the mitochondria of adult neurons can extend the life span in the fly by decreasing mitochondrial ROS production and attenuation of oxidative damage (51). We found that cells expressing hUCP4 exhibited reduced mitochondrial Ca^{2+} uptake and ROS formation compared with control cells after store depletion with TG. Cells expressing hUCP4 also exhibited resistance to the toxicity of ceramide, a trigger of store depletion and activation of the SOCE pathway (32), which has been implicated in the degeneration of neurons in AD and related neurodegenerative disorders (52). Excessive production

of ceramide may kill cells by triggering the mitochondrial-dependent pathway of apoptosis. The ability of hUCP4 to protect cells against ceramide-induced death therefore suggests an important role for this UCP in pathological conditions that involve ceramide-mediated cell death.

Grp78 is an ER chaperone that plays a critical role in maintaining cell viability under conditions of ER stress (34, 53). However, the decreased susceptibility of cells expressing hUCP4 to store depletion-induced death was not due to an effect on expression of Grp78, because the magnitude of induction of Grp78 was similar in VT and hUCP4 cells. The size of the releasable ER Ca^{2+} pool was also similar in VT and hUCP4 cells, ruling out the possibility that this parameter played a pivotal role in determining vulnerability to store depletion-induced death (36). On the other hand, we found that the rapid and sustained increase in Gadd153 protein level in response to ER store depletion was attenuated in hUCP4 cells. Gadd153 is a transcription factor that forms heterodimers with members of the CAAT/enhancer-binding protein family and is thought to be responsible for the induction of genes required for cell cycle arrest and apoptosis (54). The level of Gadd153 is very low under basal conditions, but its levels increase greatly in response to DNA damage and ER stress (54–56). Previous studies have shown that TG and ionophores induce transcriptional activation of Gadd153 by elevating $[Ca^{2+}]_i$ (35), and induction of Gadd153 may be required for release of cytochrome *c* from mitochondria and caspase activation (57). Gadd153 expression is also induced by oxidative stress (40–42), and the age-related increase in Gadd153 expression is correlated with heightened sensitivity to oxidant injury (58). Increased Gadd153 expression also mediates dopaminergic death following intrastriatal injection of 6-hydroxydopamine (59), a hydroxylated dopamine analogue that is readily oxidized causing oxidant injury. It remains to be determined whether the neuroprotective action of UCP2 in a mouse model of Parkinson disease (60) involves the suppression of Gadd153 induced by 1-methyl-4-phenylpyridinium (61). Because store depletion produces oxidative stress, which in turn induces Gadd153 expression, and because store depletion-induced death was significantly reduced by knockdown of Gadd153 expression, our data suggest that hUCP4 may contribute to the cytoprotective effect by reducing the up-regulation of oxidative stress-inducible and pro-apoptotic genes.

Collectively, our data provide evidence that hUCP4 can regulate Ca^{2+} homeostasis and signaling, apparently by reducing mitochondrial membrane potential and Ca^{2+} sequestration, the latter process playing an important role in SOCE. hUCP4 expression did not affect Bcl-2 expression but did reduce store depletion-induced oxidative stress and Gadd153 expression. Because ER stress, whether it results from protein misfolding and aggregation or from ischemic injury, inevitably leads to Ca^{2+} store depletion (62), enhancing neuronal UCP function may prove to be a valuable protective strategy to counteract mitochondrial Ca^{2+} overload and loss of mitochondrial function that precedes neurodegeneration. Future studies will determine if abnormalities in UCP4 expression or function contribute to the dysfunction and degeneration of neurons in acute and chronic neurodegenerative disorders.

REFERENCES

1. Pecqueur, C., Couplan, E., Bouillaud, F., and Ricquier, D. (2001) *J. Mol. Med.* **79,** 48–56
2. Kim-Han, J. S., Reichert, S. A., Quick, K. L., and Duga, L. L. (2001) *J. Neurochem.* **79,** 658–668
3. Bechmann, I., Diano, S., Warden, C. H., Cartfai, T., Nitsch, R., and Horvath, T. L. (2002) *Biochem. Pharmacol.* **64,** 363–367
4. Sullivan, P. G., Dube, C., Dorenbos, K., Steward, O., and Baram, T. Z. (2003) *Ann. Neurol.* **54,** 711–717
5. Mattiasson, G., Shamloo, M., Gido, G., Mathi, K., Tomasevic, G., Yi, S., Warden, C. H., Castilho, R. F., Melcher, T., Gonzalez-Zulueta, M., Nikolich, K., and Wieloch, T. (2003) *Nat. Med.* **9,** 1062–1068
6. Mao, W., Yu, X. X., Zhong, A., Li, W., Brush, J., Sherwood, S. W., Adams, S. H., and Pan, G. (1999) *FEBS Lett.* **443,** 326–330
7. Mattson, M. P., LaFerla, F. M., Chan, S. L., Leissring, M. A., Shepel, P. N., and Geiger, J. D. (2000) *Trends Neurosci.* **23,** 222–229
8. Berridge, M. J., Bootman, M. D., and Roderick, H. L. (2003) *Nat. Rev. Mol. Cell Biol.* **4,** 517–529
9. Putney, J. W., Jr. (1986) *Cell Calcium* **1,** 1–12
10. Dolmetsch, R. E., and Lewis, R. S. (1994) *J. Gen. Physiol.* **103,** 365–388
11. Negulescu, P. A., Shastri, N., and Cahalan, M. D. (1994) *Proc. Natl. Acad. Sci. U. S. A.* **91,** 2873–2877
12. Clapham, D. E., Runnels, L. W., and Strubing, C. (2001) *Nat. Rev. Neurosci.* **2,** 387–396
13. Parekh, A. B., and Putney, J. W., Jr. (2005) *Physiol. Rev.* **85,** 757–810
14. Zhang, S. L., Yu, Y., Roos, J., Kozak, J. A., Deerinck, T. J., Ellisman, M. H., Stauderman, K. A., and Cahalan, M. D. (2005) *Nature* **437,** 902–905
15. Peinelt, C., Vig, M., Koomoa, D. L., Beck, A., Nadler, M. J., Koblan-Huberson, M., Lis, A., Fleig, A., Penner, R., and Kinet, J. P. (2006) *Nat. Cell Biol.* **8,** 771–773
16. Hoth, M., Fanger, C. M., and Lewis, R. S. (1997) *J. Cell Biol.* **137,** 633–648
17. Makowska, A., Zablocki, K., and Duszynski, J. (2000) *Eur. J. Biochem.* **267,** 877–884
18. Gilabert, J. A., and Parekh, A. B. (2000) *EMBO J.* **19,** 6401–6407
19. Glitsch, M. D., Bakowski, D., and Parekh, A. B. (2002) *EMBO J.* **21,** 6744–6754
20. Gunter, T. E., Buntinas, L., Sparagna, G., Eliseev, R., and Gunter, K. (2000) *Cell Calcium* **28,** 285–296
21. Starkov, A. A., Polster, B. M., and Fiskum, G. (2002)) *J. Neurochem.* **83,** 220–228
22. Beatrice, M. C., Palmer, J. W., and Pfeiffer, D. R. (1980) *J. Biol. Chem.* **255,** 8663–8671
23. Chan, S. L., Fu, W., Zhang, P., Cheng, A., Lee, J., Kokame, K., and Mattson, M. P. (2004) *J. Biol. Chem.* **279,** 28733–28743
24. Diano, S., Matthew, R. T., Patrylo, P., Yang, L., Beal, M. F., Barnstable, C. J., and Horvath, T. L. (2003) *Endocrinology* **144,** 5014–5021
25. Jacobson, J., and Duchen, M. R. (2002) *J. Cell Sci.* **115,** 1175–1188
26. Liu, D., Chan, S. L., Slevin, J. R., DeSouza-Pinto, N. C., Wersto, R. P., Zhang, M. Mattson, M. P. (2006) *Neuromol. Med* **8,** 389–414
27. Vanden Abeele, F., Skryma, R., Shuba, Y., Van Coppenolle, F., Slomianny, C., Roudbaraki, M., Mauroy, B., Wuytack, F., and Prevarskaya, N. (2002) *Cancer Cell* **1,** 169–179
28. Pinton, P., Ferrari, D., Magalhaes, P., Schulze-Osthoff, K., Di Virgilio, F., Pozzan, T., and Rizzuto, R. (2000) *J. Cell Biol.* **148,** 857–862
29. Chen, R., Valencia, I., Zhong, F., McColl, K. S., Roderick, H. L., Bootman, M. D., Berridge, M. J., Conway, S. J., Holmes, A. B., Mignery, G. A., Velez, P., and Distelhorst, C. W. (2004) *J. Cell Biol.* **166,** 193–203
30. Wu, X., Zagranichnaya, T. K., Gurda, G. T., Eves, E. M., and Villereal, M. L. (2004) *J. Biol. Chem.* **279,** 43392–43402
31. Tesfai, Y., Brereton, H. M., and Barritt, G. J. (2001)) *Biochem. J.* **358,** 717–726
32. Minta, A., Kao, J. P., and Tsien, R. Y. (1989) *J. Biol. Chem.* **264,** 8171–8178
33. Kirichok, Y., Krapivinsky, G., and Clapham, D. E. (2004) *Nature* **427,** 360–364
34. Li, W. W., Alexandre, S., Cao, X., and Lee, A. S. (1993)) *J. Biol. Chem.* **268,** 12003–12009
35. Choi, A. M., Tucker, R. W., Carlson, S. G., Weigand, G., and Holbrook,

N. J. (1994) *FASEB J.* **8,** 1048–1054
36. Pinton, P., Ferrari, D., Rapizzi, E., Di Virgilio, F., Pozzan, T., and Rizzuto, R. (2001) *EMBO J.* **20,** 2690–2701
37. Chang, W.-C., and Parekh, A. B. (2004) *J. Biol. Chem.* **279,** 29994–29999
38. Leslie, C. C. (1997) *J. Biol. Chem.* **272,** 16709–16712
39. Cocco, T., Di Paola, M., Papa, S., and Lorusso, M. (1999) *Free Radic. Biol. Med.* **27,** 51–59
40. Guyton, K. Z., Xu, Q., and Holbrook, N. J. (1996) *Biochem. J.* **314,** 547–554
41. Carriere, A., Carmona, M. C., Fernandez, Y., Rigoulet, M., Wenger, R. H., Penicaud, L., and Casteilla, L. (2004) *J. Biol. Chem.* **279,** 40462–40469
42. Oh-Hashi, K., Maruyama, W., and Isobe, K. (2001) *Free Radic. Biol. Med.* **30,** 213–221
43. Malli, R., Frieden, M., Trenker, M., and Graier, W. F. (2005) *J. Biol. Chem.* **280,** 12114–12122
44. Varadi, A., Cirulli., V., and Rutter, G. A. (2004) *Cell Calcium* **36,** 499–508
45. Soboloff, J., and Berger, S. A. (2002) *J. Biol. Chem.* **277,** 13812–13820
46. Iijima, T., Mishima, T., Akagawa, K., and Iwao, Y. (2003) *Brain Res.* **993,** 140–145
47. Nagy, G., Koncz, A., and Perl, A. (2003) *J. Immunol.* **171,** 5188–5197
48. Crompton, M., and Costi, A. (1998) *Eur. J. Biochem.* **178,** 489–501
49. Arsenijevic, D., Onuma, H., Pecqueur, C., Raimbault, S., Manning, B. S., Miroux, B., Couplan, E., Alves-Guerra, M. C., Goubern, M., Surwit, R., Bouillaud, F., Richard, D., Collins, S., and Ricquier, D. (2000) *Nat. Genet.* **26,** 435–439
50. Negre-Salvayre, A., Hirtz, C., Carrera, G., Cazenave, R., Troly, M., Salvayre, R., Penicaud, L., and Casteilla, L. (1997) *FASEB J.* **11,** 809–815
51. Fridall, Y. C., Sanchez-Blanco, A., Silvia, B. A., and Helfand, S. L. (2005) *Cell Metab.* **1,** 145–152
52. Cutler, R. G., Kelly, J., Storie, K., Pedersen, W. A., Tammara, A., Hatanpaa, K., Troncoso, J. C., and Mattson, M. P. (2004) *Proc. Natl. Acad. Sci. U. S. A.* **101,** 2070–2075
53. Yu, Z., Luo, H., Fu, W., and Mattson, M. P. (1999) *Exp. Neurol.* **155,** 302–314
54. Luethy, J. D., Fargnoli, J., Park, J. S., Fornace, A. J., Jr., and Holbrook, N. J. (1990) *J. Biol. Chem.* **265,** 16521–16526
55. Abcouwer, S. F., Schwarz, C., and Meguid, R. A. (1999) *J. Biol. Chem.* **274,** 28645–28651
56. Milhavet, O., Martindale, J. L., Camandola, S., Chan, S. L., Gary, D. S., Cheng, A., and Mattson, M. P. (2002) *J. Neurochem.* **83,** 673–681
57. Tombal, B., Denmeade, S. R., Gillis, J. M., and Isaacs, J. T. (2002) *Cell Death Differ.* **9,** 561–573
58. Ikeyama, S., Wang, X. T., Li, J., Podlutsky, A., Martindale, J. L., Kokkonen, G., van Huizen, R., Gorospe, M., Holbrook, N. J. (2003) *J. Biol. Chem.* **278,** 16726–16731
59. Silva, R. M., Ries, V., Oo, T. F., Yarygina, O., Jackson-Lewis, V., Ryu, E. J., Lu, P. D., Marciniak, S. J., Ron, D., Przedborski, S., Kholodilov, N., Greene, L. A., and Burke, R. E. (2005) *J. Neurochem.* **95,** 974–986
60. Andrews, Z. B., Horvath, B., Barnstable, C. J., Elsworth, J., Yang, L., Beal, M. F., Roth, R. H., Matthews, R. T., and Horvath, T. L. (2005) *J. Neurosci.* **25,** 184–191
61. Conn, K. J., Gao, W. W., Ullman, M. D., McKeon-O'Malley, C., Eisenhauer, P. B., Fine, R. E., and Wells, J. M. (2002) *J. Neurosci. Res.* **68,** 755–760
62. Pachen, W. (2001) *Cell Calcium* **29,** 1–11

Mitochondrial Uncoupling Protein-4 Regulates Calcium Homeostasis and Sensitivity to Store Depletion-induced Apoptosis in Neural Cells

Sic. L. Chan, Dong Liu, George A. Kyriazis, Pamela Bagsiyao, Xin Ouyang and Mark P. Mattson

J. Biol. Chem. 2006, 281:37391-37403.
doi: 10.1074/jbc.M605552200 originally published online October 11, 2006
